

Electronic Supplementary Information

Synthesis and Characterization of a U/Pu Mixed-Actinide Microparticulate Reference Material

Bryan J. Foley,^a Spencer M. Scott,^a Michael G. Bronikowski,^a Wendy W. Kuhne,^a Kyle M. Samperton,^a Ashlee R. Swindle,^a George S. King,^a Thomas C. Shehee,^a Jonathan H. Christian,^{†a} Benjamin E. Naes,^b Travis J. Tenner,^b Matthew S. Wellons^{*a}

Savannah River National Laboratory, South Carolina, USA

Los Alamos National Laboratory, New Mexico, USA

[†] Current Affiliation for J.H.C. – Helicon Chemical Company

* Matthew.Wellons@srnl.doe.gov

Table of Contents

1.0 Purification And Characterization of Reactor-Grade Plutonium	4
2.0 Purification and Characterization of ²⁴⁰ Pu Endmember.....	6
3.0 Uranium Feedstock Preparation Details.....	7
3.1 C112A Preparation:.....	7
3.2 CRM U930D Preparation:	7
3.3 CRM U970 Preparation	7
3.4 Ternary Uranium Solution Mixing	7
3.5 Uranyl Oxalate Synthesis	8
4.0 Mixed Uranium/Plutonium Feedstock Mixing	9
5.0 UV-Vis Pu Stability Study.....	10
6.0 Representative Particle Nearest Neighbor Plots	13
7.0 Aerodynamic Particle Size Measurements.....	14
8.0 Alpha Spectroscopy Measurements and SEM Correlation	17
9.0 LG-SIMS Independently Bias Corrected ²³⁵ U/ ²³⁸ U and ²⁴⁰ Pu/ ²³⁹ Pu Isotope Amount Ratios..	19
9.1 Introduction and Methods.....	19
9.2 Results and Comparison to RM UPu-100A Values	19
9.2.1 LG-SIMS independently bias corrected ²³⁵ U/ ²³⁸ U isotope amount ratio	19
9.2.2 LG-SIMS independently bias corrected ²⁴⁰ Pu/ ²³⁹ Pu isotope amount ratio	20

1.0 Purification And Characterization of Reactor-Grade Plutonium

Inside a radiological glovebox, approximately 5 g of aged reactor-grade plutonium oxide¹ was dissolved in 102 mL of 12 M HNO₃ containing ~10 mmol KF at ~108 °C. Complete dissolution required approximately 24 hours. This plutonium nitrate solution was vacuum filtered through a cellulose nitrate filter to remove any insoluble debris in the source material. The acid concentration of the filtrate was adjusted from 12 M to 8 M by addition of deionized water. The resultant plutonium concentration in solution was approximately 16 g/L.

To achieve an efficacious purification, two molar equivalents of ferrous sulfamate were added to reduce all Pu^{IV,V,VI} to Pu^{III}; this reduction was verified by UV-Vis spectroscopy. The combination of self-radiolytic oxidation and a small amount of NaNO₂ to the 8 M HNO₃ solution was sufficient to re-oxidize Pu³⁺ back to Pu^{IV} with minimal to no Pu^V or Pu^{VI} detected in solution. This valence adjustment is critical as only Pu^{IV} yields the anion Pu(NO₃)₆²⁻ which is retained by the resin at high acid concentrations.

Commercially purchased Reillex® HPQ anion-exchange resin was converted from the chloride form (as-shipped) to the nitrate form by washing with 1 M NaNO₃.² After conversion, the nitrate-exchanged resin was loaded into an SRNL-fabricated glass column with a 19-mm inner diameter. A representative diagram of the purification setup is shown in Figure A. The total resin bed volume was ~106 mL.

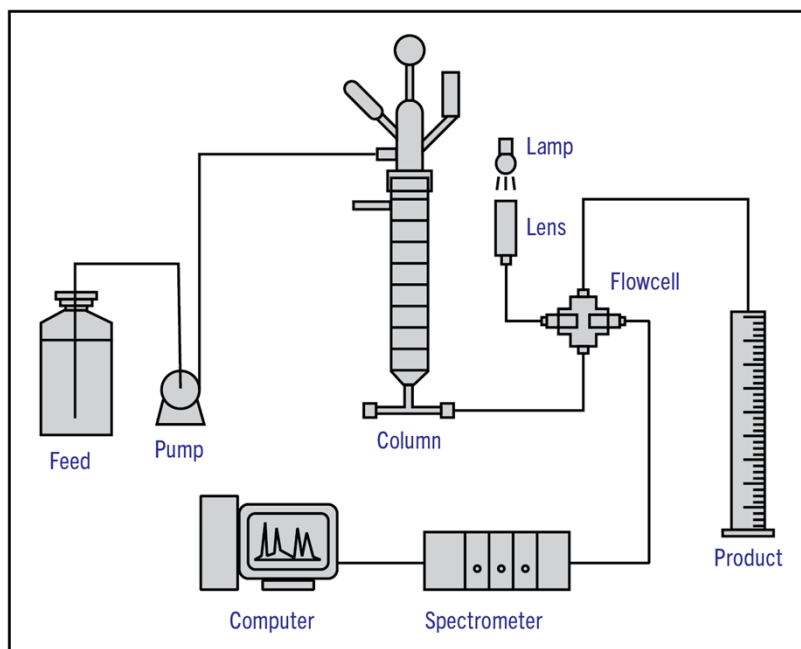


Figure A. Schematic of the chromatography setup used to purify solutions of plutonium nitrate.

A spectroscopic flow cell was composed of a ¼" Swagelok® cross and two ¼" optic lenses with a 3.36-mm path length was attached to the outlet of the column (Figure B). Two pairs of fiber optic lines installed through the ceiling of the glovebox allowed a light signal to be transmitted into the glovebox and passed through the flow cell and carried out to an Avantes AVS Rack Mount USB2

spectrometer controlled by a computer. The flow cell and spectrometer were used to monitor the eluate upon exit from the column to maximize Pu collection efficiency.

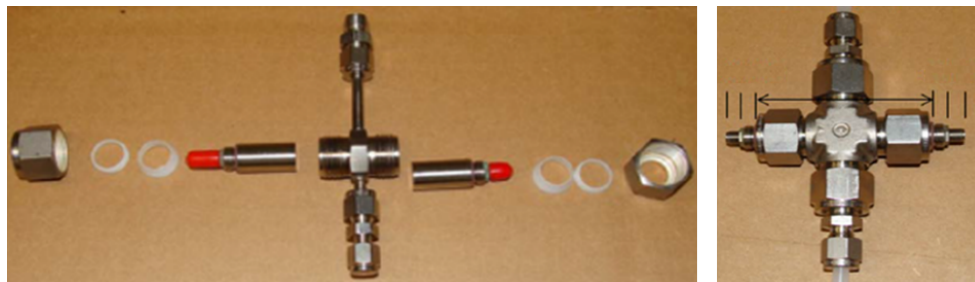


Figure B. Left: Disassembled spectroscopic flow cell used to monitor eluate during anion-exchange purification. Right: The assembled spectroscopic flow cell.

The resin was conditioned with ~100 mL of 8 M HNO_3 (~1 bed volume). The Pu^{IV} feed solution was then loaded onto the column at a rate of ~4 mL/min yielding a green band at the top of the resin bed. The loaded column was washed with 1 L of 8 M HNO_3 at a rate between 4 and 12 mL/min. This washing process separated the plutonium loaded on the column from other species in solution which have little or no affinity for the resin. The eluate from the washing step was monitored using the spectroscopic flow cell to ensure that plutonium was not inadvertently exiting the column.

After passing 1 L of 8 M HNO_3 through the column, the feed solution was changed to a 0.35 M HNO_3 solution. Reducing the nitric acid concentration neutralizes the $\text{Pu}(\text{NO}_3)_6^{2-}$ anion through conversion to $\text{Pu}(\text{NO}_3)_4$ thereby releasing Pu from the anion exchange resin. The 0.35 M HNO_3 was pumped through the column at a rate of 6 mL/min and the eluent was collected in three fractions. The spectroscopic flow cell and visual confirmation of the resin color were used to determine when the three fractions should be collected.

The first fraction (“displacement”) contained 96 mL of column eluate. This fraction contained HNO_3 , residual impurities from the rinse step, and minimal Pu.

The second fraction (“hearts”) contained 155 mL of column eluate. This fraction contained majority of the eluted Pu.

The third fraction (“tails”) contained 155 mL of column eluate. This fraction contained mostly dilute HNO_3 and residual Pu.

Aliquots of each fraction were submitted for analysis by ICP-OES, ICP-MS, and gamma spectroscopy. The final hearts fraction existed as a ~1 M nitric acid solution containing approximately 4.7 grams of Pu. Plutonium comprised 99.7 weight percent (wt%) of the elements in solution. The next highest remaining impurity was ^{232}Th at 0.13 wt% in solution. All other impurities in solution comprised less than 0.17% combined.

2.0 Purification and Characterization of ^{240}Pu Endmember

The manipulations performed in purifying the ^{240}Pu source material were nearly identical as those described above with the exception that the sourced ^{240}Pu was a 4-gram purification instead of the 5-gram quantity described for the reactor-grade plutonium purification. The same bed of Reillex® HPQ resin was used for both purifications. As such, all column parameters, flow rates, spectroscopic monitoring, and method by which column fractions were collected were identical to those described above.

As above, aliquots of the displacement, hearts, and tails fractions were submitted for analysis by ICP-OES, ICP-MS, and gamma spectroscopy. The final hearts fraction existed as a ~1 M nitric acid solution containing approximately 4.2 grams of Pu. Plutonium comprised 98.9 wt% of the elements in solution. The highest remaining impurity was ^{237}Np at 0.89 wt% in solution. All other impurities in solution comprised less than 0.2% combined.

3.0 Uranium Feedstock Preparation Details

Uranium endmembers for RM UPu-100A were calculated using the SRNL AMOS mixing algorithm. The selected endmembers are shown in Table A. Mixing parts provided by the AMOS software are parts by uranium element weight in each CRM.

Table A. Mixing parts calculated by the AMOS mixing algorithm for the uranium endmembers.

	C112A	U930D	U970
Mixing Parts	9570	317	113
Mixing Percentages	95.7	3.2	1.1

3.1 C112A Preparation:

C112A was treated in accordance with the directions on the C112A certificate. In short, the uranium metal was soaked in 8 M HNO_3 for approximately 15 minutes to remove surface oxidation. The metal piece was then rinsed with deionized water followed by a rinse with acetone. The metal was weighed immediately after the acetone evaporated. The metal was then placed into an 8 M HNO_3 solution where it was allowed to dissolve to completion over the course of several days. This uranyl nitrate solution was quantitatively transferred to an HNO_3 -leached, fluorinated ethylene propylene (FEP) bottle where it was stored until used for mixing operations.

3.2 CRM U930D Preparation:

U930D was received as seven individual quantities of approximately 5.4 grams of an estimated 1 mg/g uranyl nitrate solution in glass ampules. These ampules were opened, and their contents were quantitatively transferred into an HNO_3 -leached FEP bottle. The total mass of the solution transferred to the FEP bottle was 36.55 g with an approximate concentration of 1 mg of U per gram of solution per the NBL certificate.

3.3 CRM U970 Preparation

CRM U970 was received as bulk triuranium octoxide, U_3O_8 , per the NBL certificate. The black powder was placed in a quartz crucible and weighed. The crucible was then placed in a muffle furnace and heated to 120 °C for two hours to remove any surface-adsorbed water followed by 2 hours at 800 °C to convert any lower oxides (e.g., UO_2 , UO_3 , etc.) of uranium to U_3O_8 . After cooling to ambient temperature, the crucible was weighed again. The final mass of the U970 in the quartz crucible was 0.95 of the original mass, indicating a 5% reduction in mass from dehydration of surface water from the U_3O_8 powder. The requisite amount of U970 as determined by the AMOS mixing calculation was weighed into a FEP bottle and dissolved by the addition of 8 M HNO_3 .

3.4 Ternary Uranium Solution Mixing

CRM U970 and CRM U930D were mixed first, according to the mixing directions provided by the AMOS mixing algorithm. An aliquot of this solution was removed and analyzed by MC-ICP-MS to ensure that the resulting uranium isotopic composition was appropriate before continuing. Once the desired isotopic distribution was confirmed, the necessary quantity of CRM112A solution was determined and then added gravimetrically to an HNO_3 -leached glass vial. After placing the

requisite solution mass in the vial, the CRM 112A solution was quantitatively added to the U930D/U970 mixture, which produced the ternary uranium solution needed for U/Pu microparticle fabrication.

3.5 Uranyl Oxalate Synthesis

The ternary uranium solution was transferred into a HNO_3 -leached glass beaker and heated to 50–60 °C for several hours to reduce the volume by half and raise the uranium concentration to above 50 g/L. While maintaining a solution temperature of 50–60 °C, a solution of oxalic acid (10.0 mL of a 0.5 M solution in ultrapure water; 1.05 eq.) was added dropwise to the beaker over the course of 15 minutes. The reaction mixture was removed from the heat and the allowed to cool for 30 minutes. During this time, a yellow precipitate formed in the beaker. The beaker containing the uranium precipitate was placed into an ice bath for 20 minutes to facilitate additional precipitation. These solids were isolated by vacuum filtration and stored in a desiccator over CaSO_4 (Drierite) until the morning of U/Pu microparticle production.

4.0 Mixed Uranium/Plutonium Feedstock Mixing

In a radiological glovebox on the morning of production, an aliquot of uranyl oxalate trihydrate was dissolved in a sufficient quantity of nitric acid such that the resulting concentration of uranium in solution was 2.04 mM. Specifically, for the particles shown in this report, 19.3 mg of uranyl oxalate trihydrate was dissolved in 22.681 mL of 0.1 M HNO_3 .

Meanwhile, an aliquot of the binary plutonium mixture was diluted to 2.04 mM using 0.1 M HNO_3 as a diluent. These two solutions were combined volumetrically in a 1:100 ^{239}Pu : ^{238}U ratio. An aliquot of this solution was removed for analysis by Q-ICP-MS. After particle production, a second aliquot was removed from the feedstock solution to ensure solution stability and purity was maintained throughout the production process. A graphical representation of the feedstock mixing process is shown in Figure C.

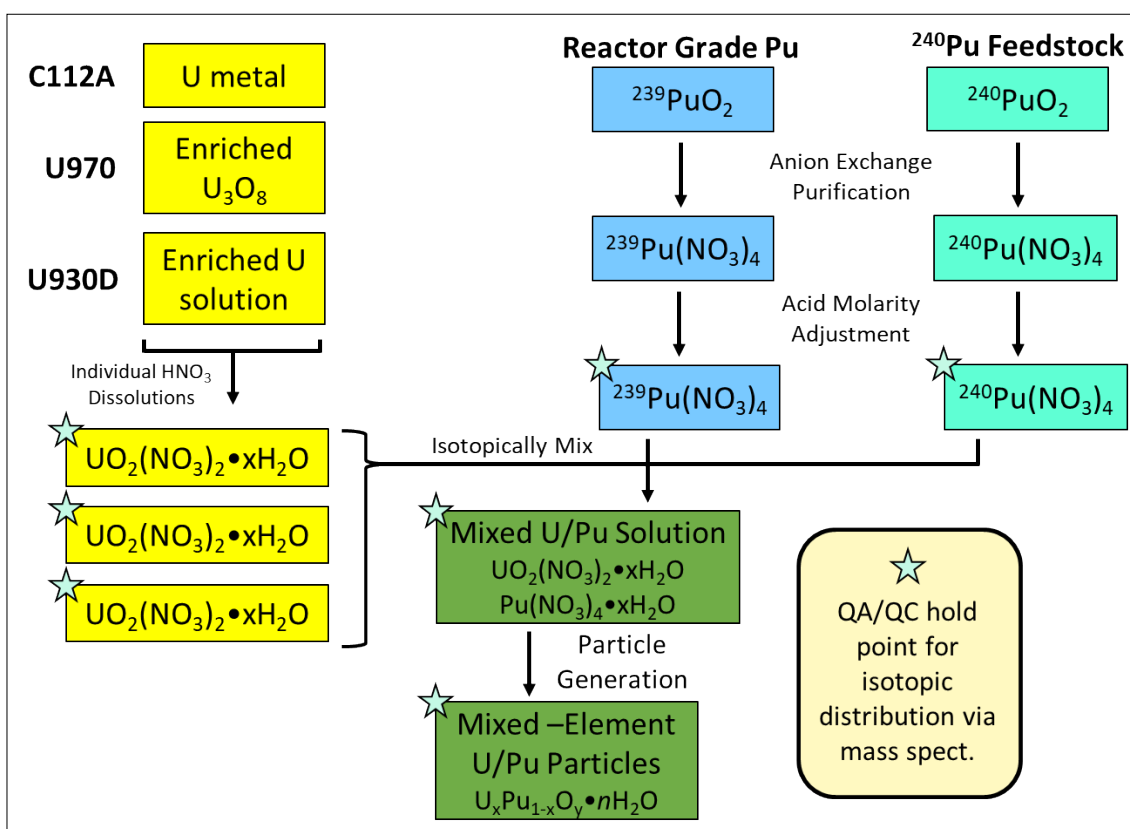


Figure C. Graphical representation of the isotopic mixing process required to prepare mixed actinide U/Pu particles. Isotopes listed for Pu endmembers are the isotope with the highest atomic percent in each material.

5.0 UV-Vis Pu Stability Study³

Inside the radiological glovebox, a cuvette holder was attached to the fiber optic lines of the Avantes AVS Rack Mount USB2 spectrometer described in the chromatographic purification section. A variety of plutonium solutions were prepared to determine if there were any suitable conditions which would prevent plutonium colloidal particle formation while also minimizing changes to the feedstock matrix which may impact aerosol particle formation. A representative UV-Vis spectrum of $\text{Pu}(\text{NO}_3)_4$ decomposing in ultrapure water is shown in Figure D.

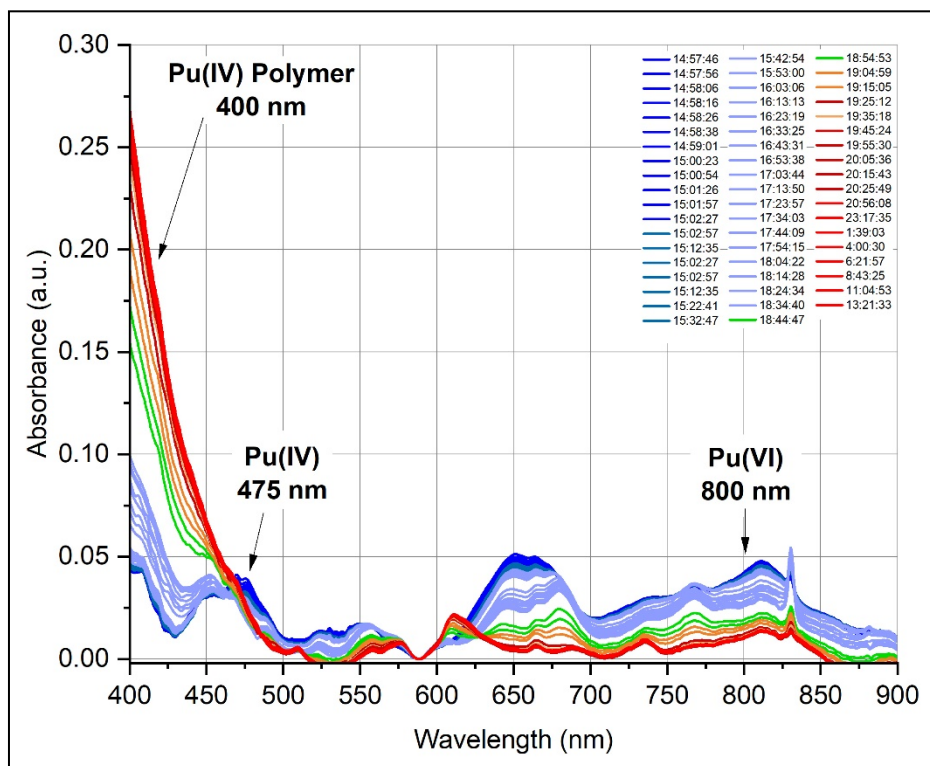


Figure D. Representative time-lapse UV-Vis spectra acquired on a $\text{Pu}(\text{NO}_3)_4$ solution in ultrapure water over 24 hours. Notable timepoints: dark blue is $T = 0$ hours, green is $T = 3$ hours, and Red is $T = 24$ hours.

The plutonium polymer absorption band is centered in the UV and only the tail of the band can be seen in Figure C. However, of note is that before the cuvette can be closed and inserted into the holder, plutonium polymeric species can be observed in the UV-Vis spectrum. The band related to these colloidal species continually gets larger over time. Attempts at varying the plutonium concentration with a constant feedstock matrix (ultrapure water) yielded no satisfactory difference in the rate of formation of the plutonium colloidal particle formation. Further, neither changing the order of addition [water into $\text{Pu}(\text{NO}_3)_4$ vs. $\text{Pu}(\text{NO}_3)_4$ into water] nor slowing the rate of addition of one into the other changed the result of colloidal particle formation. In each case, a series of spectra similar to the one shown in Figure D was obtained.

Addition of nitric acid to the diluent was the next tested variable. Dilution of $\text{Pu}(\text{NO}_3)_4$ using 0.1 M HNO_3 as a diluent did not yield any detectable quantity of colloidal plutonium particle formation Figure E.

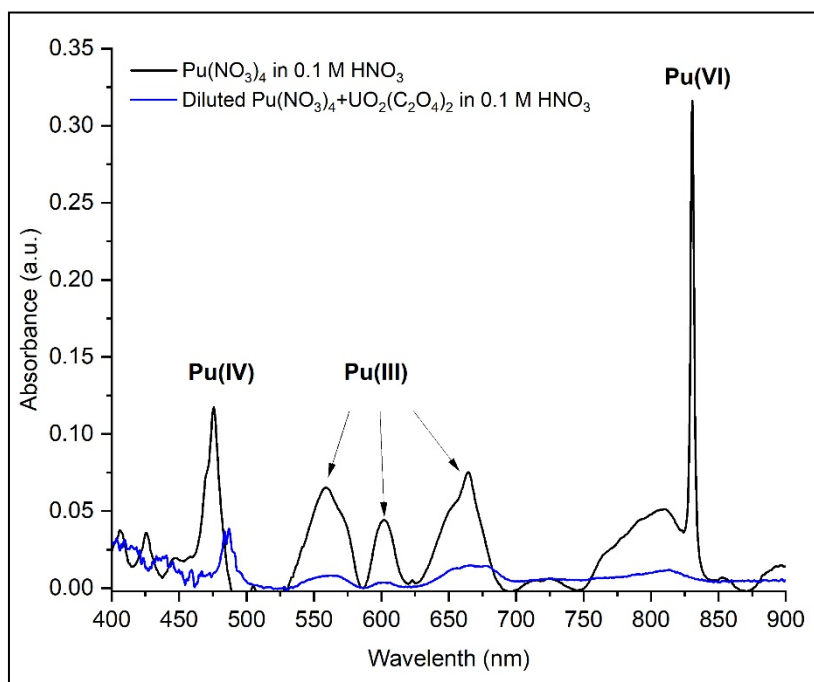


Figure E. UV-Vis spectrum of a $\text{Pu}(\text{NO}_3)_4$ solution diluted in 0.1 M HNO_3 (black trace) and UV-Vis spectrum of a diluted $\text{Pu}(\text{NO}_3)_4$ feedstock solution in 0.1 M HNO_3 containing ~2mM $\text{UO}_2(\text{C}_2\text{O}_4)_2$ (blue trace).

The black trace in Figure E is the result of diluting $\text{Pu}(\text{NO}_3)_4$ in 0.1 M HNO_3 . The tail of the band corresponding to plutonium colloidal particle formation is not visible, indicating that the acidification of the feedstock solution has effectively stabilized the Pu in solution. Increasing the complexity of the solution to more closely resemble the RM UPu-100A microparticle feedstock still does not yield any obvious degradation products that would warrant further reformulation. A new band does emerge in the UV-Vis spectrum of this mixture at 487 nm. We assume that the new band could arise from an oxalate-bridged mixed-U/Pu complex formed in situ;⁴ however, no attempts were made to ascertain the origin of the new UV-Vis band and the chemical species which gave rise to the band did not negatively impact particle formation.

Attempting to lower the acid content of the feedstock to 0.03 M yielded colloidal plutonium polymer formation in as little as two hours as shown in Figure F. As such, a feedstock HNO_3 concentration of 0.1 M was used for the entirety of the RM UPu-100A microparticle production process.

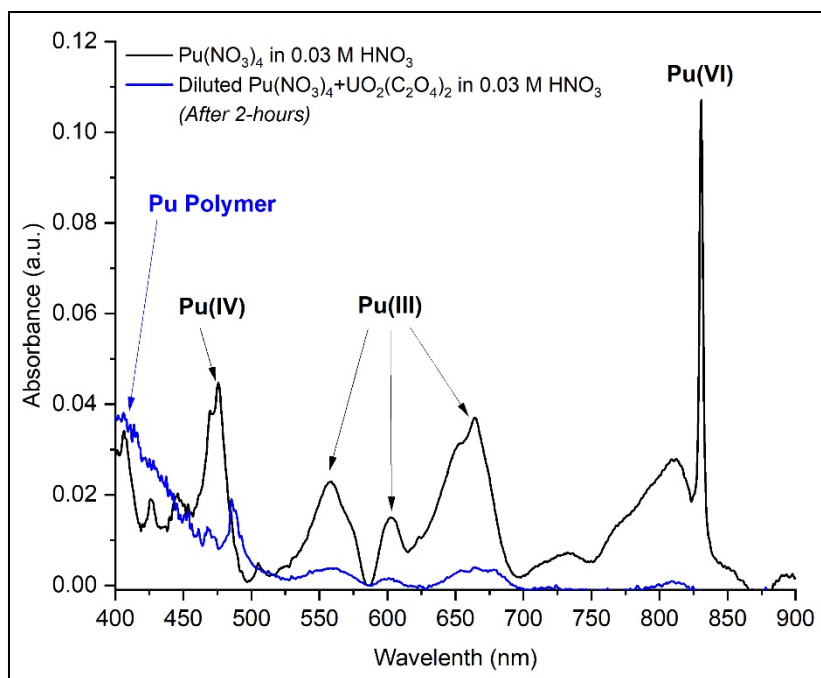


Figure F. UV-Vis spectrum of a $\text{Pu}(\text{NO}_3)_4$ solution diluted in 0.03 M HNO_3 (black trace) and UV-Vis spectrum of a diluted $\text{Pu}(\text{NO}_3)_4$ feedstock solution in 0.03 M HNO_3 containing ~2mM $\text{UO}_2(\text{C}_2\text{O}_4)_2$ (red trace).

6.0 Representative Particle Nearest Neighbor Plots

Scanning electron microscopy (SEM) automated particle mapping (APM) was performed for 13 RM UPu-100A plachets and the position data for each particle was recorded. Nearest neighbor calculations and plots were made for seven of the plachets. Six of these plots are found in Figure G. The apparent ring of particles (most notable on the lower left plot) is actually the laser-scribed ring on the silicon plachet and appears due to the SEM APM settings necessary to resolve the particles; this analytical artifact produces a statistically insignificant number of false-positive particle detections.

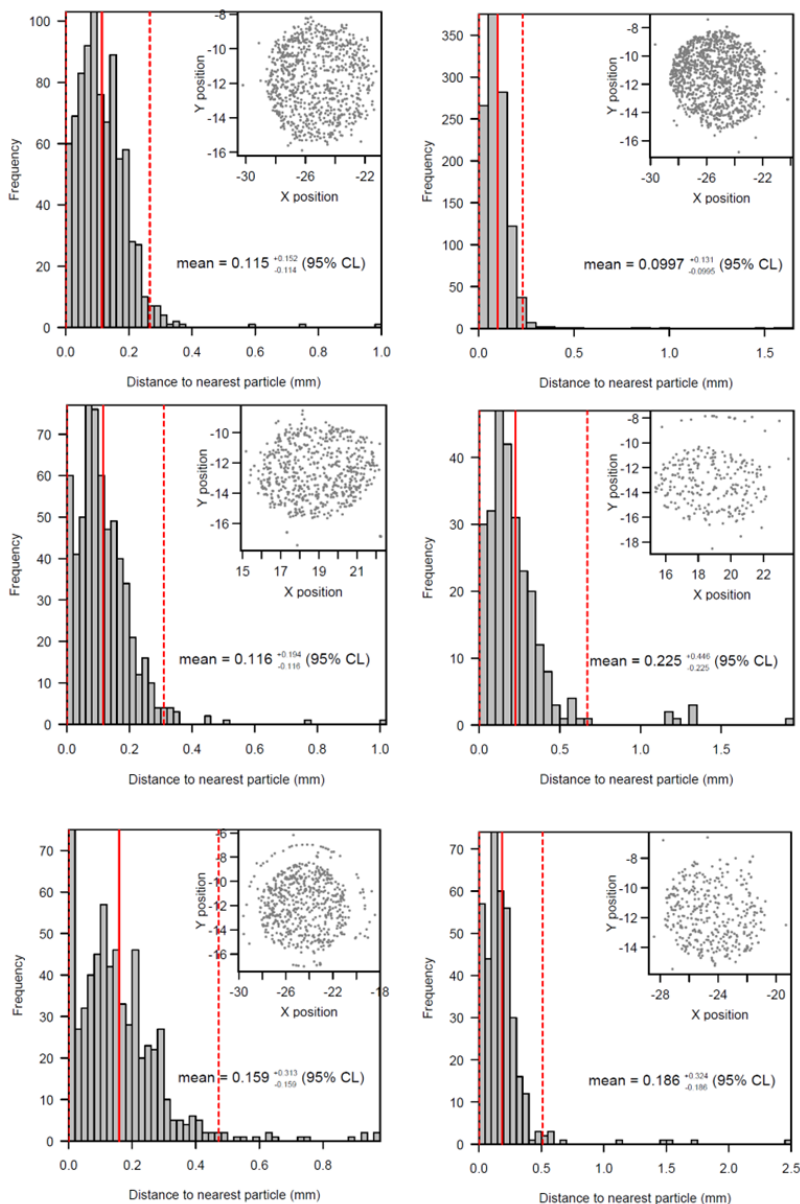


Figure G. Representative histograms showing the typical distance between particles (in mm) across six of the measured U/Pu particulate-laden plachets.

7.0 Aerodynamic Particle Size Measurements

The size uniformity of the generated particles was assessed throughout production by periodic aerodynamic particle size measurements, with a standard deviation of 1.8% between the average values of the 50 measurements made throughout the duration of the 3.1-hour particle production. Distributions of particle sizes measured by APS throughout the production are shown in Figure H.

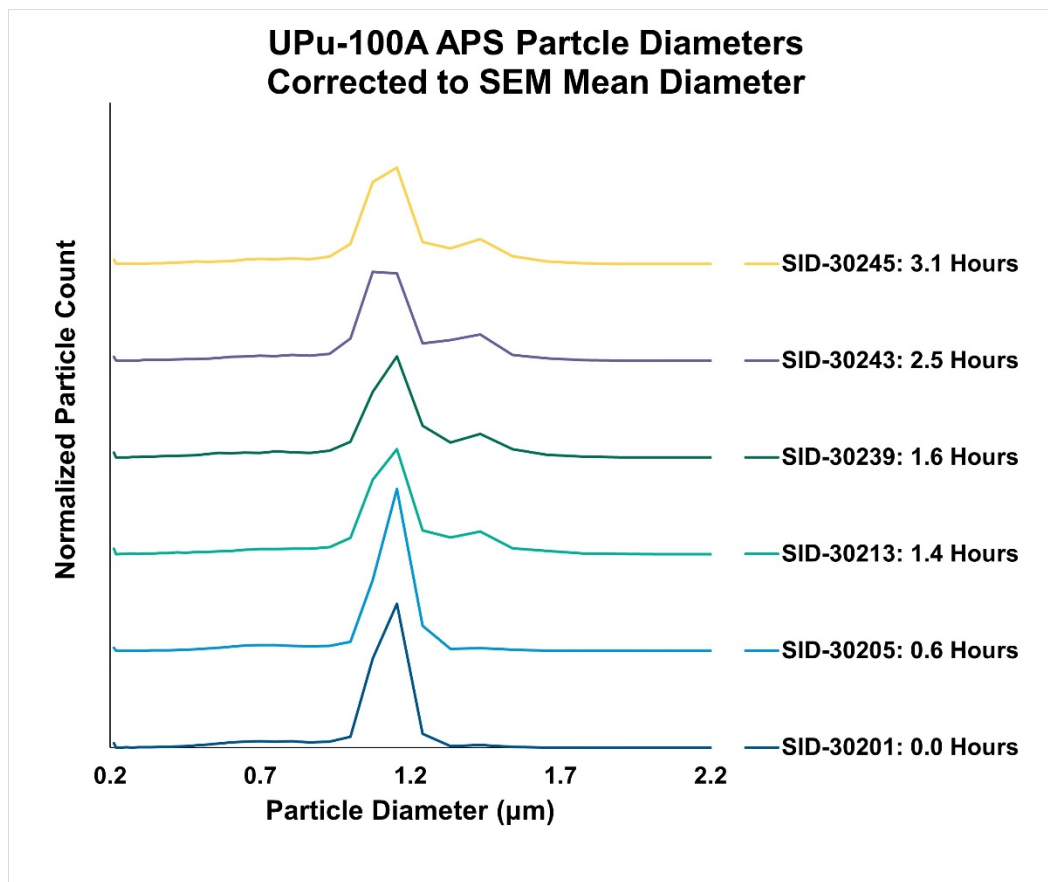


Figure H. Normalized frequency distribution of the U/Pu particle size (μm) as determined by aerodynamic particle sizing and corrected by mean particle diameter measured by SEM APM shown at different times during THESEUS particle production. Plots have been shifted vertically so that features of each plot are apparent. The peak that grows in at a higher particle size with time is due to coalescence of two droplets in the aerosol stream (“doublet”).

8.0 Alpha Spectroscopy Measurements and SEM Correlation

Alpha spectra were acquired on 90 different planchets laden with the produced U/Pu microparticles. A representative alpha spectrum is shown in Figure I. SEM APA was performed on 13 of these planchets. By correlating the total background subtracted alpha activity (Bq) to the number of U-bearing particles identified by SEM APA, a correlation was established between alpha activity and particle loading (Figure J). One caveat with this method of determining particle loading is that this correlation identifies alpha emitting radioisotopes only so it was necessary to only count SEM-APM particles that contained uranium. The number of non-U/Pu particles on the planchets were quantified by SEM APM and EDS analysis which showed that on average, non-U/Pu materials constituted <4% of the population. Non-U/Pu particles identified by EDS were iron- (2.7%) and nickel-bearing (2.1%). While the origin of these non-U/Pu contaminants was not determined, the flight path of the particles include Swagelok® valving and the planchets were handled with metal tweezers (Ted Pella), both potential sources of said particles.

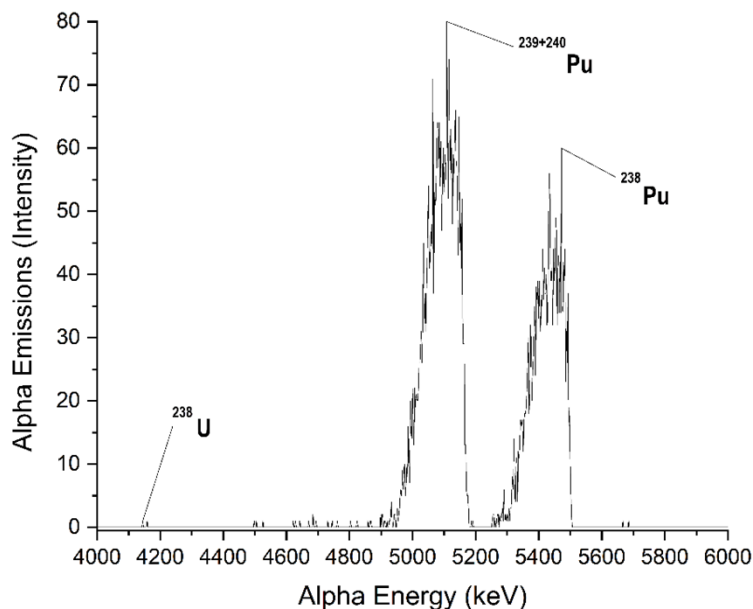


Figure I. Representative alpha energy spectrum of RM UPu-100A measured by alpha pulse height analysis.

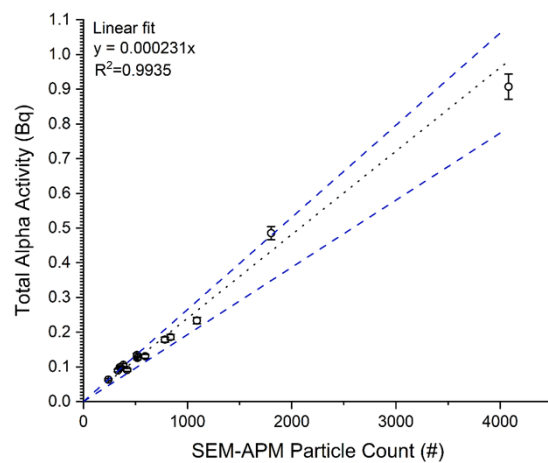


Figure J. Correlation of total alpha activity and SEM APA particle counts from 13 planchets measured by both techniques.

9.0 LG-SIMS Independently Bias Corrected $^{235}\text{U}/^{238}\text{U}$ and $^{240}\text{Pu}/^{239}\text{Pu}$ Isotope

Amount Ratios

9.1 Introduction and Methods

In addition to the LG-SIMS single particle consumption analyses detailed in the main text, a second set of single particle data was collected where $n(^{235}\text{U})/n(^{238}\text{U})$ and $n(^{240}\text{Pu})/n(^{239}\text{Pu})$ values were independently bias corrected (i.e., calibrated), and particles were only partially consumed. Specifically, analyses were only 150 seconds in duration, split into ten 15-second cycles. The same beam conditions were applied as with the complete particle consumption analyses, with the exception that a sputter cleaning step of 150 seconds in duration was employed.

Instrument bias corrections were made using bracketing measurements of U_3O_8 certified reference material (CRM) U030 particles to correct raw $n(^{235}\text{U})/n(^{238}\text{U})$ values, and bracketing measurements of particles from the Nuclear Forensics International Technical Working Group (ITWG) sixth collaborative materials exercise (CMX-6)^{5,6} that contain Pu, were used to correct raw $n(^{240}\text{Pu})/n(^{239}\text{Pu})$ values. Regarding the CMX-6 material, a working reference $n(^{240}\text{Pu})/n(^{239}\text{Pu})$ value of 0.06172 ± 0.00007 was used, which was derived from the weighted mean value of replicate MC-ICP-MS analyses⁷ with the uncertainty representing a propagated error combining (1) the expanded standard deviation (2SD) of the replicate values, and (2) the uncertainty of the CRM 126-A material used to calibrate the MC-ICP-MS instrument. The CMX-6 reference $n(^{240}\text{Pu})/n(^{239}\text{Pu})$ value is decay corrected to June 30, 2023, which is the date that LG-SIMS data were collected from the RM UPu-100A planchets. From June 30, 2023, to the date of the RM UPU-100A MC-ICP-MS data collection (September 1, 2023), the additional decay of ^{239}Pu and ^{240}Pu is sufficiently small that it does not affect the isotope ratios to the reported significant figures.

Uncertainties of individual data are reported as twice the standard error (2SE) of the isotope compositions from the ten cycles per analysis. For single particle datasets, the weighted mean values of isotope compositions are reported, using the inverse of individual data uncertainties as the weighting factor. Uncertainties of dataset weighted mean values are propagated, combining (1) the expanded standard deviation (2SD) of the dataset, as a relative uncertainty; and (2) the uncertainty of the corresponding reference material (e.g., CRM U030, CMX-6), as a relative uncertainty.

9.2 Results and Comparison to RM UPu-100A Values

9.2.1 LG-SIMS independently bias corrected $^{235}\text{U}/^{238}\text{U}$ isotope amount ratio

For the independently bias corrected $n(^{235}\text{U})/n(^{238}\text{U})$ dataset, the weighted mean value is 0.05205 ± 0.00023 ($k=2$), Figure K. This value is in agreement with the RM UPu-100A $n(^{235}\text{U})/n(^{238}\text{U})$ value defined for this material (0.05221 ± 0.00024). Homogeneity of the measured values was evaluated using a counting statistics model⁸ of the expected dispersion of the data about the mean value due to counting statistics at the 99.99% confidence level ($k=4$). The dataset exhibits

isotope homogeneity in $n(^{235}\text{U})/n(^{238}\text{U})$ when compared to the counting statistics-based model (red curves in Figure K).

9.2.2 LG-SIMS independently bias corrected $^{240}\text{Pu}/^{239}\text{Pu}$ isotope amount ratio

For the independently bias corrected $n(^{240}\text{Pu})/n(^{239}\text{Pu})$ dataset, the weighted mean value is 0.2817 ± 0.0025 ($k=2$), Figure L. This value agrees with the RM UPu-100A $n(^{240}\text{Pu})/n(^{239}\text{Pu})$ value (0.2838 ± 0.0032) within the uncertainty. The dataset exhibits isotope homogeneity in $n(^{240}\text{Pu})/n(^{239}\text{Pu})$ when compared to the counting statistics-based model (red curves in Figure L).

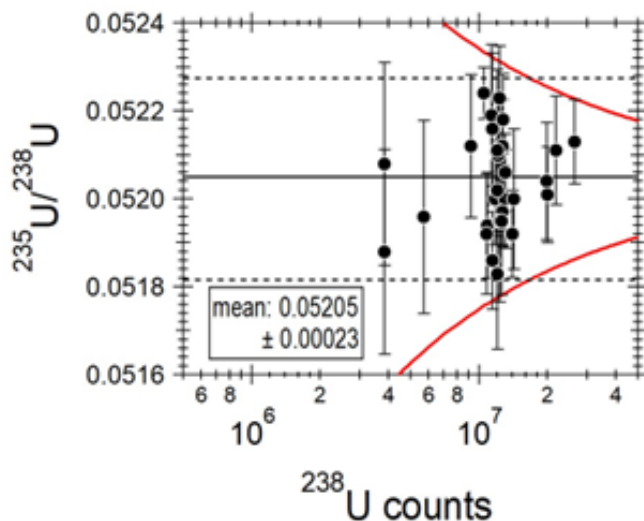


Figure K. LG-SIMS independently bias corrected data and models of homogeneity for $n(^{235}\text{U})/n(^{238}\text{U})$. Dashed lines are the uncertainty of the weighted mean value and red curves are the counting statistics-based model prediction of data scatter about the mean assuming the material is isotopically homogeneous.

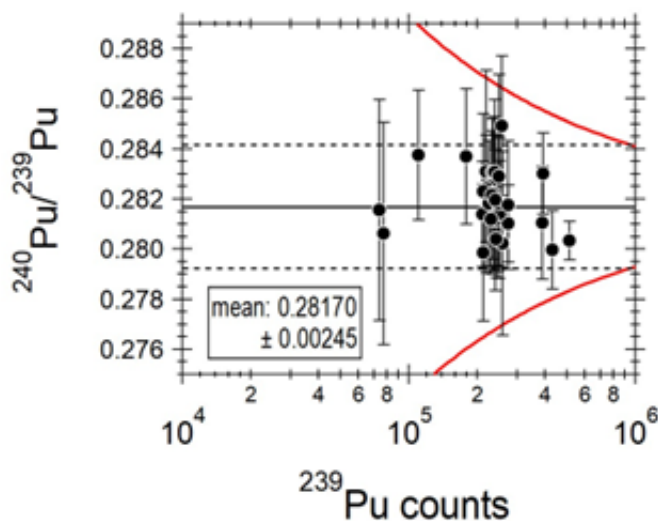


Figure L. LG-SIMS independently bias corrected data and models of homogeneity for $n(^{240}\text{Pu})/n(^{239}\text{Pu})$. Dashed lines are the uncertainty of the weighted mean value and red curves are the counting statistics-based model prediction of data scatter about the mean assuming the material is isotopically homogeneous.

Supporting Information References

1 Duffey, J. M.; Veirs, D. K.; Berg, J. M.; Livingston, R. R. Pressure Development in Sealed Containers with Plutonium-bearing Materials. In *Journal of Nuclear Materials Management*, 2010.

2 Steimke, J. L.; Williams, M. R.; Steeper, T. J.; Leishear, R. A. "Nitrate Conversion of HB-Line Reillex™ HPQ Resin", SRNL-STI-2012-00160, May 2012, <https://sti.srs.gov/fulltext/SRNL-STI-2012-00160.pdf>.

3 For detailed studies on spectrochemical and electrochemical investigations of plutonium nitrate solutions, see: a) Chatterjee, S.; Peterson, J. M.; Casella, A. J.; Levitskaia, T. G.; and Bryan, S. A. *Inorg. Chem.* **2020**, *59*, 6826-6838. b) Lines, A. M.; Adami, S. R.; Casella, A. J.; Sinkov, S. I.; Lumetta, G. J.; Bryan, S. A. *Electroanalysis* **2017**, *29*, 2744.

4 Tamain, C.; Chapelet, B. A.; Rivenet, M.; Abraham, F.; Caraballo, R.; Grandjean, S. Crystal Growth and First Crystallographic Characterization of Mixed Uranium(IV)–Plutonium(III) Oxalates. *Inorganic Chemistry* **2013**, *52*, 4941-4949.

5 Schwantes J.M., Corbey J.F. and Marsden O. (2022) Exercise Celestial Skónis: Part 1- History, purpose, design, and results of traditional forensic examinations of the 6th Collaborative materials exercise of the nuclear forensics International Technical Working Group. *Forensic Chemistry* 29, doi:10.1016/j.forc.2022.100424.

6 Schwantes J.M., Corbey J.F. and Marsden O. (2022) Exercise Celestial Skónis: Part 2- Emerging technologies and State of Practice of nuclear forensic analyses demonstrated during the 6th collaborative materials exercise of the nuclear forensics International Technical Working Group. *Forensic Chemistry* 29, doi:10.1016/j.forc.2022.100423.

7 Kayzar-Boggs T.M., Xu N., Aragon S.M., Auxier J.D. II, Boswell M., Chamberlin R.M., Denton J.S., Dry D.E., Garduno K., Hansen S.M.K., Hudston L.A., Knaak M.A., Kinman W.S., Kuhn K.J., Lente J.L., Lujan E.J.W., Mathew K.J., Mayo R.J., Meininger D., Montoya D.P., Pacheco S.D., Pike R., Pollington A., Rearick M., Schappert M., Scott B., Shorty M., Steiner R., Tenner T., Tew E., Wayne D., Wende A., Williamson T., Worley C., Wylie E.M., Yost D. (2019) Los Alamos National Laboratory CMX-6 60 Day Report Case ID 369X-HQ-CMX6/2018-CMX6. pp. 1-83. LA-UR-19-24382.

8 Tenner, T. J.; Naes, B. E.; Wurth, K. N.; Meininger, D.; Wellons, M.; Pope, T. R. New Particle Working Standards for NWAL Particle Laboratory Calibration and Quality Control – LANL LG-SIMS Characterization and Evaluation. In Proceedings from the INMM & ESARDA Joint Annual Meeting 2023.